Springer

KSME

Journal of Mechanical Science and Technology 24 (12) (2010) 2451~2460
www.springerlink.com/content/1738-494x
DOI 10.1007/s12206-010-0920-4

Unsteady thin airfoil theory revisited for a general deforming airfoil †

Christopher O. Johnston[1], William H. Mason[1] and Cheolheui Han[2,*]

[1]*Department of Aerospace and Ocean Engineering, Virginia Polytechnic Institute and State University, Blacksburg, VA 24060, USA*
[2]*Department of Aeronautical and Mechanical Design Engineering, Chungju National University, 50 Daehak-Ro, Choongbuk, 380-702, Korea*

(Manuscript Received January 29, 2010; Revised July 21, 2010; Accepted October 11, 2010)

Abstract

The unsteady thin airfoil theory of von Karman and Sears is extended to analyze the aerodynamic characteristics of a deforming airfoil. The von Karman and Sears approach is employed along with Neumark's method for the unsteady load distribution. The wake-effect terms are calculated using either the Wagner or Theodorsen function, depending on the desired camberline deformation. The concept of separating the steady and damping terms in the camberline boundary condition is introduced. The influence of transient and sinusoidal airfoil deformations on the airfoil load distribution is examined. The general equations developed for the unsteady lift and load distribution are evaluated analytically for a morphing airfoil, which is defined here by two quadratic curves with arbitrary coefficients. This general camberline is capable of modeling a wide range of practical camberline shapes, including leading and trailing edge flaps. Results of the present model are shown for a variable camber, or morphing, airfoil configuration. The influence of transient and sinusoidal motion on the force coefficients and load distribution is addressed.

Keywords: Morphing airfoil; Thin airfoil theory; Von Karman and Sears approach; Unsteady aerodynamics

1. Introduction

A fundamental problem in applied aerodynamics concerns the prediction of the time-history of the aerodynamic forces acting on an airfoil following a change in the airfoil geometry [1]. Recent interest in morphing control devices, which produce a hingless change to the airfoil camber, has led to the possibility of camberline shape changes other than just a conventional hinged flap [2, 3]. The aerodynamic forces acting on the airfoil during and after the change in shape have an influence on both the actuator design and aircraft dynamics [4, 5]. Because of the large variety of possible shape changes for a morphing airfoil, it is desirable to formulate the problem in a theoretical framework that provides insight into the unsteady response of the aerodynamic forces to a general change in airfoil shape. A valid approach for this task is the classical unsteady thin airfoil theory developed by Theodorsen [6] and von Karman and Sears [7]. Although such a classical technique contains many approximations (inviscid, incompressible, small disturbances) and one may obtain more accurate results from widely available numerical approaches, the benefit of being able to separate various components of the unsteady load distribution or force and moment coefficients provides insight into the problem, which may then be confirmed through more advanced methods. Thus, the unsteady thin airfoil theory warrants consideration.

There have been many applications of unsteady thin airfoil theory applied to trailing edge flaps reported in the literature [6-16], and since the trailing edge flap is a special case of the general deforming camberline discussed later in this paper, these studies have particular relevance to the present problem. One of the earliest of these studies, the well known application to a harmonically oscillating trailing edge flap by Theodorsen's [6] provided the lift and pitching moment characteristics of the airfoil. Although Theodosen also presented results for the flap hinge moments, no results were given for the airfoil load distributions. Postel and Leppert [8], along with a number of German researchers (Dietze [9-11], Jaekel [12], Schwarz [13, 14], and Sohngen [15, 16]) determined the load distribution on a harmonically oscillating airfoil. Recently, Mateescu and Abdo [17] obtained both the unsteady forces and the load distribution using the method of velocity singularities. Narkiewicz et al. [18] solved a similar problem which allowed for arbitrary flap and airfoil oscillations. Lieshman [19] and Hariharan and Lieshman [20] considered arbitrary flap deflections using indicial concepts, although both focused mainly on the compressible flow case.

Although there has been considerable research on the theoretical unsteady aerodynamics of a trailing edge flap, there has been little research concerning other deforming camberline

† This paper was recommended for publication in revised form by Associate Editor Do Hyung Lee

* Corresponding author. Tel.: +82 -11-9143-3574, Fax.: +82 -43-841-5370
E-mail address: chhan@cjnu.ac.kr

Table 1. Geometric coefficients for specific camberlines represented by Eq. (24).

	A_1	B_1	C_1	A_2	B_2	C_2
(a) Trailing-edge (TE) flap	0	0	0	0	-1	x_B
(b) Leading-edge (LE) flap	0	1	$-x_B$	0	0	0
(c) Conformal TE flap	0	0	0	$\frac{1}{2(x_B-1)}$	$\frac{x_B}{(1-x_B)}$	$\frac{x_B^2}{2(x_B-1)}$
(d) Conformal LE flap	$-\frac{1}{2x_B}$	1	$-\frac{x_B}{2}$	0	0	0
(e) NACA 4-digit (Config. A)	$-\frac{1}{x_B^2}$	$\frac{2}{x_B}$	0	$-\frac{1}{(1-x_B)^2}$	$\frac{2x_B}{(1-x_B)^2}$	$\frac{(1-2x_B)}{(1-x_B)^2}$
(f) NACA 4-digit (Config. A)	$-\frac{1}{x_B^2}$	$\frac{2}{x_B}$	-1	$-\frac{1}{(1-x_B)^2}$	$\frac{2x_B}{(1-x_B)^2}$	$-\frac{x_B^2}{(1-x_B)^2}$

Table 2. Camberlines Represented by Eq. (24) and Table 1.

TE Flap	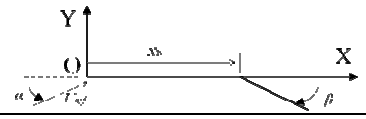
LE Flap	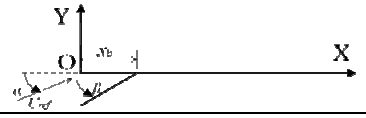
Conformal TE Flap	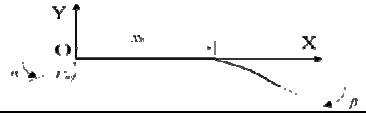
Conformal LE Flap	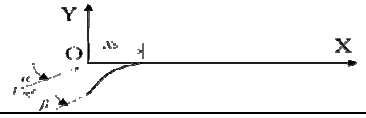
NACA 4-digit (Config. A)	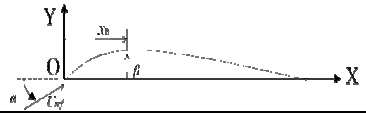
NACA 4-digit (Config. B)	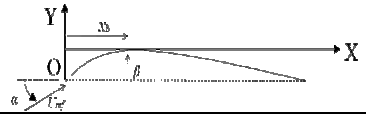

shapes. Schwarz [13, 14] studied an oscillating parabolic control surface. This shape was meant to account for the viscous effects of a conventional flap by smoothing out the hinge line. Recent interest in morphing aircraft has created interest in this parabolic, or conformal flap, for use as a hingless control surface [21, 22]. Unfortunately, the previous work of Schwarz [13, 14] has gone unnoticed in the English-speaking literature except for the brief mention by Garrick [23] and the discussion in the translated article by Schwarz [14]. Spielburg [24] studied the unsteady aerodynamics of an airfoil with an oscillating parabolic camberline. This study was restricted to a circular arc parabolic camberline, which was meant to represent chordwise aeroelastic deformations. Mesaric and Kosel [25] determined the lift and pitching moment for cubic polynomial camberlines. No mention was made of the load distribution. Singh [26] and Maclean [27] presented a numerical model for the unsteady aerodynamics of deforming airfoils, although they did not discuss the agreement of their methods with theory. Other sources of information regarding the modeling of deforming camberlines are the theoretical studies of membrane airfoils. For example, Llewelyn [28] and Boyd [29, 30] discuss the application of steady thin airfoil theory to various single-segment polynomial camberlines, which are similar to those of interest for morphing applications.

The aim of this paper is to outline a systematic application of unsteady thin airfoil to a "general deforming camberline", which will be composed o two parabolic curves. This shape has the ability to model a wide variety of camberline shapes, and it can be reduced to a conventional trailing edge flap. This feature is convenient for validation and for illustrating the differences of the trailing edge flap with other more complicated configurations. For the quasi-steady force coefficient and load distribution calculation, the present method combines the approaches of Glauret [32] and Allen [33]. The von Karman and Sears'approach [7] for the unsteady force coefficient calculation is adopted along with Neumark's method [34] for the unsteady load distribution. The wake-effect terms are calculated using either the Wagner or Theodorsen function. The influence of transient and sinusoidal airfoil deformations on the airfoil load distribution are examined. It should be noted that a feature of the present study is the analytic determination of the unsteady load distribution for the general deforming camberline. This has not been presented previously in the literature.

2. Unsteady thin airfoil method

Considering the incompressible small disturbance flow around a two dimensional thin airfoil, von Karman and Sears [7] represented the lift and the pitching moment in terms of the following three components: quasi-steady, apparent mass and wake induced. Their results are based on the coordinate system with its origin fixed to the mid-chord and with its x-axis set parallel to the chord. The origin of the coordinate system in the present method is set to the leading edge with its x-axis parallel to the chord (See Table 2). Applying the transformation $x=(1-\cos\theta)c/2$ to von Karman and Sears' results, the three (quasi-steady, apparent mass, wake-induced) components of the lift are written as follows:

$$L_0 = \rho U \Gamma_0 \quad \text{(1a)} \tag{1a}$$

$$L_1 = \frac{\rho c^2}{4}\frac{\partial}{\partial t}\left(\int_0^{\pi}\gamma_0(\theta)\cos\theta\sin\theta d\theta\right) \quad \text{(1b)} \tag{1b}$$

$$L_2 = \frac{\rho U c}{2}\int_c^{\infty}\frac{\gamma(\xi)}{\sqrt{\xi^2-\xi}}d\xi \quad \text{(1c)} \tag{1c}$$

where Γ_0 and γ_0 are the quasi-steady circulation and vorticity

values, respectively, and $\gamma(\xi)$ is the vorticity in the wake at the location ξ. It is convenient to represent γ_0 using Glauert's Fourier series [32] which is written as

$$\gamma_0(\theta,t) = 2U\left(A_0(t)\left[\frac{1+\cos\theta}{\sin\theta}\right] + \sum_{n=1}^{\infty} A_n(t)\sin n\theta \right) \quad (2)$$

where $A_0 = -\int_0^{\pi} w(\theta,t)d\theta/\pi$ and $A_n = 2\int_0^{\pi} w(\theta,t)\cos(n\theta)d\theta/\pi$. In these equations, w is the downwash that is used to impose the instantaneous boundary condition for no flow through the camberline. For a time-varying camberline defined by z_c, the downwash, w, is written as

$$w = \frac{1}{U}\frac{\partial z_c}{\partial t} + \frac{\partial z_c}{\partial x}. \quad (3)$$

Substituting Eq. (3) into Eqs. (1) and (2) leads to the following equations for the quasi-steady and apparent mass contributions to the lift

$$L_0 = \rho U^2 c\pi(A_0 + A_1/2) \quad (4a)$$

$$L_1 = \frac{\rho c^2 U}{8}\pi(2\dot{A}_0 + \dot{A}_2). \quad (4b)$$

Note that the dot above the A_0 and A_2 in Eq. (4b) indicates the time-derivative of the coefficient, which actually indicates a time derivative of w only since the rest of the equation is independent of time.

The unsteady pressure distribution is formulated in terms of the equations presented by Neumark [34], which conveniently correspond to the three lift components presented in Eq. (1). Applying the transformation $x = (1-\cos\theta)c/2$ to Δp_0 (quasi-steady component) and Δp_1 (apparent mass component) and Δp_2 (wake induced component) in [34] results in

$$\Delta p_0 = \rho U\gamma_0(\theta) = 2\rho U^2\left(A_0\left[\frac{1+\cos\theta}{\sin\theta}\right] + \sum_{n=1}^{\infty} A_n \sin n\theta \right) \quad (5a)$$

$$\Delta p_1 = \rho\frac{c}{2}(d/dt)\int_0^{\theta}\gamma_{0n}(\theta)\sin\theta \; d\theta \quad (5b)$$

$$\Delta p_2 = \frac{\rho U}{\pi}\sqrt{\frac{c-x}{x}}\int_c^{\infty}\frac{\gamma(\xi)}{\sqrt{\xi^2-\xi}}d\xi. \quad (5c)$$

These equations require that the circulatory (γ_{0c}) and non-circulatory (γ_{0n}) quasi-steady vorticity distributions be defined. From Neumark [34], γ_{0c} and γ_{0n} may be written as

$$\gamma_{0c}(\theta) = \frac{2\Gamma_0}{\pi c\sin\theta} \quad (6a)$$

$$\gamma_{0n}(\theta) = \frac{2U}{\pi\sin\theta}\int_0^{\pi}\frac{w(\theta_0,t)\sin^2\theta_0}{\cos\theta_0-\cos\theta}d\theta_0 \quad (6b)$$

where $\Gamma_0 = 2Ub\int_0^{\pi} w(\theta,t)\sqrt{(1-\cos\theta)/(1+\cos\theta)}\sin\theta d\theta$. The quasi-steady circulation strength (Γ_0) in Eq. (6a) is obtained by integrating Eq. (2) across the chord, which results in the following

$$\Gamma_0 = \pi cU\left(A_0 + \frac{A_1}{2}\right). \quad (7)$$

Substituting this equation for Γ_0 into Eq. (6a) results in $\gamma_{0c}(\theta) = U(2A_0 + A_1)/\sin\theta$. Similarly, the noncirculatory component of the vorticity distribution (γ_{0n}) may be written as

$$\gamma_{0n}(\theta) = 2UA_0\frac{\cos\theta}{\sin\theta} - UA_1\frac{1}{\sin\theta} + \frac{2U}{\pi}\int_0^{\pi}\frac{w(\theta_0,t)\sin\theta}{\cos\theta_0-\cos\theta}d\theta_0. \quad (8)$$

Substituting Eq. (8) into Δp_1 in Eq. (5b) and performing the integration results in

$$\Delta p_1 = \rho_{\infty}\frac{c}{2}(d/dt)[2UA_0\sin\theta - UA_1\theta + \int_0^{\theta}\gamma_b(\theta)\sin\theta \; d\theta \;] \quad (9)$$

where the basic load distribution (γ_b) is defined as $\gamma_b(\theta) = \frac{2U}{\pi}\int_0^{\pi}\frac{w(\theta_0,t)\sin\theta}{\cos\theta_0-\cos\theta}d\theta_0$.

For many practical applications, the function z, which defines the camberline shape, can be represented in the following form:

$$z(x,\tau) = \psi(x)\beta(\tau) \quad (10)$$

where ψ defines the form of the camberline (for example a flapped or a parabolic camberline) and β defines the time varying magnitude of the camberline (for example the flap deflection angle or magnitude of maximum camber) as a function of the nondimensional time ($\tau = U_{\infty}t/c$). This form for z will be used throughout the remainder of this paper.

To identify the aerodynamic forces resulting from the steady camberline slope and the unsteady camberline shape change, w will be written in general as

$$w = \frac{\partial z}{\partial x} + \frac{1}{c}\frac{\partial z}{\partial \tau} = w_s + w_d \quad (11)$$

where w_s is the "steady" component ($w_s = \frac{\partial\psi}{\partial x}\beta$) which and is proportional to β and w_d is the "damping" component ($w_d = \frac{\psi}{c}\frac{\partial\beta}{\partial\tau}$) which is proportional to $d\beta/d\tau$. Both w_s and w_d result in their own quasi-steady circulation components ($\Gamma_{0,s}$ and $\Gamma_{0,d}$), which consequently result in their own apparent-mass and wake-effect components through Eq. (5b) and (5c). Therefore, the terminology of "steady" and "damping", denoted by a subscript s and d, will be used throughout this paper to distinguish between lift or pressure components resulting from w_s and w_d, respectively. Using this concept, the quasi-steady lift (L_0) and apparent mass lift (L_1) can be written

in terms of the lift components due to the camber (β), the camberline shape-change with time (β'), and camberline shape-change acceleration (β'') as follows:

$$\frac{L_0}{qc} = C_{L,0} = \frac{1}{qc}\frac{dL_0}{d\beta}\beta + \frac{1}{qc}\frac{dL_0}{d\beta'}\beta' = K_{0,s}\beta + K_{0,d}\beta' = \pi(2\bar{A}_{0,s} + \bar{A}_{1,s})\beta + \pi(2\bar{A}_{0,d} + \bar{A}_{1,d})\beta' \quad (12a)$$

$$\frac{L_1}{qc} = C_{L,1} = \frac{1}{qc}\frac{dL_1}{d\beta'}\beta' + \frac{1}{qc}\frac{dL_1}{d\beta''}\beta'' = K_{1,s}\beta' + K_{1,d}\beta'' = \frac{\pi}{4}(2\bar{A}_{0,s} + \bar{A}_{2,s})\beta' + \frac{\pi}{4}(2\bar{A}_{0,d} + \bar{A}_{2,d})\beta'' \quad (12b)$$

where q is the dynamic pressure, and $K_{1,s}$ and $K_{1,d}$ are the apparent mass lift components due to the time-rate-of-change of $\gamma_{0,s}$ and $\gamma_{0,d}$, respectively. The Fourier coefficients in Eq. (12) are defined as follows:

$$\bar{A}_{0,s} = -\frac{1}{\pi}\int_0^\pi \frac{\partial\psi}{\partial x}d\theta \quad (13a)$$

$$\bar{A}_{n,s} = \frac{2}{\pi}\int_0^\pi \frac{\partial\psi}{\partial x}\cos(n\theta)d\theta \quad (13b)$$

$$\bar{A}_{0,d} = -\frac{1}{\pi}\int_0^\pi \frac{\psi}{c}d\theta \quad (13c)$$

$$\bar{A}_{n,d} = \frac{2}{\pi}\int_0^\pi \frac{\psi}{c}\cos(n\theta)d\theta . \quad (13d)$$

The quasi-steady and apparent-mass load distribution can also be separated into steady and damping components as follows:

$$\frac{\Delta p_0(\theta)}{q} \equiv \Delta C_{p,0} = \frac{1}{q}\frac{d\Delta p_0}{d\beta}\beta + \frac{1}{q}\frac{d\Delta p_0}{d\beta'}\beta' = \left[\bar{A}_{0,s}\chi(\theta) + T_{0,s}(\theta)\right]\beta + \left[\bar{A}_{0,d}\chi(\theta) + T_{0,d}(\theta)\right]\beta' \quad (14a)$$

$$\frac{\Delta p_1(\theta)}{q} = \Delta C_{p,1} = \frac{d\Delta p_1}{d\beta'}\beta' + \frac{d\Delta p_1}{d\beta''}\beta'' = T_{1,s}(\theta)\beta' + T_{1,d}(\theta)\beta'' \quad (14b)$$

where the load distribution functions are defined as

$$T_{0,s}(\theta) = \frac{4}{\pi}\int_0^\pi \frac{\frac{\partial\psi}{\partial x}(\theta_0,t)\sin\theta}{\cos\theta_0 - \cos\theta}d\theta_0 \quad (15a)$$

$$T_{0,d}(\theta) = \frac{4}{\pi c}\int_0^\pi \frac{\psi(\theta_0,t)\sin\theta}{\cos\theta_0 - \cos\theta}d\theta_0 \quad (15b)$$

$$T_{1,s} \equiv \frac{1}{q}\frac{d\Delta p_1}{d\beta'} = 2\bar{A}_{0,s}\sin\theta - \bar{A}_{1,s}\theta + \frac{1}{2}\int_0^\theta T_{0,s}(\theta)\sin\theta d\theta \quad (15c)$$

$$T_{1,d} \equiv \frac{1}{q}\frac{d\Delta p_1}{d\beta''} = 2\bar{A}_{0,d}\sin\theta - \bar{A}_{1,d}\theta + \frac{1}{2}\int_0^\theta T_{0,d}(\theta)\sin\theta d\theta \quad (15d)$$

with $\chi(\theta) = 4(1+\cos\theta)/\sin\theta$. In these equations, $T_{0,s}$ and $T_{0,d}$ are steady and damping components due to the steady and damping basic load distributions, respectively. The first term in Eq. (14b) is the apparent mass term ($\Delta p_{1,s}$) due to the time-rate-of-change of $\gamma_{0,s}$, and the second term in Eq. (14b) is the damping term ($\Delta p_{1,d}$) due to the time-rate-of-change of $\gamma_{0,d}$.

Collecting the terms defined in the previous paragraphs for the quasi-steady and apparent-mass contributions to the lift and load distribution, the following equations can be written:

$$C_L = K_{0,s}\beta + (K_{0,d} + K_{1,s})\beta' + K_{1,d}\beta'' + C_{L,2} \quad (16a)$$

$$\Delta C_p = \left[\bar{A}_{0,s}\chi(\theta) + T_{0,s}(\theta)\right]\beta + \left[\bar{A}_{0,d}\chi(\theta) + T_{0,d}(\theta) + T_{1,s}(\theta)\right]\beta' + T_{1,d}(\theta)\beta'' + \Delta C_{p,2} \quad (16b)$$

where the wake-effect components ($C_{L,2}$ and $\Delta C_{p,2}$) depend on the time variation of β. For transient and sinusoidal variations of β, the wake-effect component of the lift coefficient, $C_{L,2}$, is written as follows:

$$C_{L,2}(\tau) = (K_{0,s}\Delta\beta(\tau_0) + K_{0,d}\Delta\beta'(\tau_0))\phi(\tau) + \int_{\tau_0}^{\tau}(K_{0,s}\beta'(\sigma) + K_{0,d}\beta''(\sigma))\phi(\tau - \sigma)d\sigma \quad \text{(transient)} \quad (17a)$$

$$C_{L,2} = [C(k) - 1]\left(K_{0,s}\beta + K_{0,d}\beta'\right) \quad \text{(sinusoidal)} \quad (17b)$$

where ϕ is the Wagner function and $C(k)$ is the Theodorsen function, $k = \omega c/2U$ is the reduced frequency. The Wagner function may be modeled using the approximation introduced by Jones [35], which is written as $\phi(\tau) = -0.165e^{-0.091\tau} - 0.335e^{-0.6\tau}$. The Theodorsen function is a complex number written as $C(k) = F(k) + iG(k)$. For both the transient and sinusoidal cases, the load distribution is written as follows:

$$\Delta C_{p,2} = \frac{2}{\pi}\left[\frac{1+\cos\theta}{\sin\theta}\right]C_{L,2} \quad (18)$$

where the time dependence is contained in $C_{L,2}$.

The application of Theodorsen's function to a sinusoidal oscillation of L_0 can be generalized by applying the separation of "steady" and "damping" terms defined previously to a sinusoidal oscillation of β. Consider a time-varying β defined as follows:

$$\beta = \bar{\beta}e^{i\bar{k}\tau} = \bar{\beta}\left[\cos(\bar{k}\tau) + i\sin(\bar{k}\tau)\right] \quad (19)$$

where $\bar{\beta}$ is the magnitude of the oscillation and $\bar{k} = \omega c/U$ and $\tau = Ut/c$. Note that $\bar{k}$ is defined differently than the classically defined k, where $\bar{k} = 2k$. From Eqs. (16a) and (17b), the total unsteady lift coefficient may be written for sinusoidal motion as

$$C_L(\tau) = K_{0,s}\beta + \left(K_{0,d} + K_{1,s}\right)\beta' + K_{1,d}\beta'' + [C(k) - 1]\left(K_{0,s}\beta + K_{0,d}\beta'\right) \quad (20)$$

Substituting Eq. (19) into (20) and keeping only the real part results in

$$C_L(\tau,\bar{k}) = Z_1\left(\bar{k}\right)\beta\cos\left(\bar{k}\tau\right) + Z_2\left(\bar{k}\right)\beta\sin\left(\bar{k}\tau\right) \tag{21}$$

where $Z_1\left(\bar{k}\right) = -\left[K_{1,d}\bar{k}^2 - K_{0,s}F + K_{0,d}\bar{k}G\right]$ and $Z_2\left(\bar{k}\right) = -\left[K_{1,s}\bar{k} + K_{0,s}G + K_{0,d}\bar{k}F\right]$. The lift can also be presented in terms of a magnitude and phase angle as follows:

$$C_L\left(\tau,\bar{k}\right) = \bar{C}_L\beta\cos\left(\bar{k}\tau + \phi_L\right) \tag{22}$$

where $\bar{C}_L = \sqrt{Z_1^2 + Z_2^2}$, $\phi_L = \tan^{-1}\left(-Z_2/Z_1\right)$. Likewise, the load distribution can be written as

$$\Delta C_p(\tau,\theta,\bar{k}) = \Pi_1\left(\bar{k},\theta\right)\beta\cos\left(\bar{k}\tau\right) + \Pi_2\left(\bar{k},\theta\right)\beta\sin\left(\bar{k}\tau\right) \tag{23}$$

where $\Pi_1\left(\bar{k},\theta\right) = \begin{bmatrix}\bar{A}_{0,s}\chi(\theta) + T_{0,s}(\theta) - T_{1,d}(\theta)\bar{k}^2 \\ +\dfrac{\chi(\theta)}{2\pi}\left(K_{0,s}F - K_{0,s} - \bar{k}K_{0,d}G\right)\end{bmatrix}$ and

$$\Pi_2\left(\bar{k},\theta\right) = -\begin{bmatrix}\left(\bar{A}_{0,d}\chi(\theta) + T_{0,d}(\theta) + T_{1,s}(\theta)\right)\bar{k} \\ +\dfrac{\chi(\theta)}{2\pi}\left(K_{0,s}G + \bar{k}K_{0,d}F - \bar{k}K_{0,d}\right)\end{bmatrix}.$$

3. Application to a general deforming camberline

The equation for a general camberline consisting of two quadratic segments may be written as

$$z_{c,n} = \beta(\tau)\left(a_n x^2 + b_n x + c_n\right);\ n = 1 \tag{24}$$

for $0 \le x \le x_B$ and $n = 2$ for $x_B \le x \le c$

where x_B is the location at which the two segments connect. The coefficients in Table 1 represent six basic camberline shapes of possible interest and Table 2 illustrates these shapes. Applying these definitions to Eq. (24), while also applying the transformation of $x = (1-\cos\theta)c/2$, results in the following:

$$w_{s,n} = \beta(\tau)\left(H_n\cos\theta + I_n\right) \tag{25a}$$

$$w_{d,n} = \frac{\beta'(\tau)}{c}\left(E_n\cos^2\theta + F_n\cos\theta + G_n\right) \tag{25b}$$

where $H_n = -a_n$, $I_n = a_n + b_n$, $E_n = a_n/4$, $F_n = -a_n/2 - b_n/2$, and $G_n = a_n/4 + b_n/2 + c_n$.

3.1 Quasi-steady load distribution

Having defined the steady and damping components of downwash w in Eq. (11), the quasi-steady load distribution and force coefficients may be calculated. The main challenge in obtaining the load distribution is evaluating the integral for the basic load distribution (Eq. (14)). Substituting Eq. (25) into Eq. (15) results in the following two equations for the steady and damping components of the nondimensional basic load distribution

$$T_{0,s}(\theta) = \frac{2}{\pi}\left\{\begin{matrix}\left[2(I_1 - I_2) + 2(H_1 - H_2)\cos\theta\right] \\ \times\ln\left(\dfrac{\sin\theta\tan\left(\theta_B/2\right) - \cos\theta + 1}{\sin\theta\tan\left(\theta_B/2\right) + \cos\theta - 1}\right) \\ +2\left[\theta_B H_1 + (\pi - \theta_B)H_2\right]\sin\theta\end{matrix}\right\} \tag{26a}$$

$$T_{0,d}(\theta) = \frac{2}{\pi}\left\{\begin{matrix}\left[\begin{matrix}2(G_1 - G_2) + 2(F_1 - F_2)\cos\theta \\ +(E_1 - E_2)(1 + \cos 2\theta)\end{matrix}\right] \\ \times\ln\left(\dfrac{\sin\theta\tan\left(\theta_B/2\right) - \cos\theta + 1}{\sin\theta\tan\left(\theta_B/2\right) + \cos\theta - 1}\right) \\ +2\left[\begin{matrix}\theta_B(F_1 + E_1\cos\theta) \\ +(\pi - \theta_B)(F_2 + E_2\cos\theta) \\ +(E_1 - E_2)\sin\theta_B\end{matrix}\right]\sin\theta\end{matrix}\right\}. \tag{26b}$$

Eq. (26a) may be validated for a conventional TE flap by comparing it with Spence's result [36] and for a conformal TE flap by comparing with Johnston's result [37]. For an NACA 4-digit airfoil case, Eq. (26a) can be shown to compare well with Pinkerton's approximate result [38].

As shown in Eq. (14a), the component of the quasi-steady load distribution is not dependent on $T_{0,s}$ or $T_{0,d}$, but dependent only on $\bar{A}_{0,s}$ and $\bar{A}_{0,d}$. This component of the load distribution, called the additional load distribution, has the shape of an angle of attack produced load distribution (represented by ψ). Eq. (12) shows that the quasi-steady lift depends on the first three Fourier coefficients (the fourth coefficient, $\bar{A}_{3,s}$, is calculated as well to determine $\bar{A}_{2,d}$). The steady coefficients are evaluated as follows,

$$\begin{aligned}
\bar{A}_{0,s} &= -\frac{1}{\pi}\left[I_2\left(\pi - \theta_B\right) + I_1\theta_B + \left(H_1 - H_2\right)\sin\theta_B\right] \\
\bar{A}_{1,s} &= \frac{1}{\pi}\left[\begin{matrix}H_2\left(\pi - \theta_B\right) + H_1\theta_B + \\ \left(\begin{matrix}2\left(I_1 - I_2\right) \\ +\left(H_1 - H_2\right)\cos\theta_B\end{matrix}\right)\sin\theta_B\end{matrix}\right] \\
\bar{A}_{2,s} &= \frac{2}{3\pi}\left[\begin{matrix}3\left(I_1 - I_2\right)\cos\theta_B + \\ \left(H_1 - H_2\right)\left(2 + \cos 2\theta_B\right)\end{matrix}\right]\sin\theta_B \\
\bar{A}_{3,s} &= \frac{1}{3\pi}\left[6\left(H_1 - H_2\right)\cos^3\theta_B\sin\theta_B + 2\left(I_1 - I_2\right)\sin 3\theta_B\right].
\end{aligned} \tag{27}$$

For a TE flap, these coefficients can be shown to agree with Glauert's [32] or Allen's [33] result. For the damping quasi-steady terms, only $\bar{A}_{0,d}$ must be determined because of the relationships for $\bar{A}_{1,d}$ and $\bar{A}_{2,d}$ given in Eq. (13).

3.2 Apparent mass load distribution

Examining Eq. (14b) for the apparent mass load distribution ($\Delta C_{p,I}$), it is clear that the only component not yet known is the integral term required for $T_{I,d}$ (the Fourier coefficients were required for the quasi-steady terms and $T_{I,s}$ does not need

to be determined because it is equal to $T_{0,d}$). Thus, the only required integration for $T_{1,d}(\theta)$ is the following

$$\int_0^\theta T_{0,d}(\theta)\sin\theta \; d\theta$$
$$= \frac{1}{3\pi}\left[\begin{array}{l}\left[\begin{array}{l}(3E+12G)\cos\theta_B+3(F)\cos 2\theta_B\\ +E\cos 3\theta_B\end{array}\right]\times\ln\left[-\dfrac{\sin\left(\dfrac{\theta_B+\theta}{2}\right)}{\sin\left(\dfrac{\theta_B-\theta}{2}\right)}\right]\\ -\left[\begin{array}{l}(3E+12G)\cos\theta+3(F)\cos 2\theta\\ +E\cos 3\theta\end{array}\right]\ln\left[\dfrac{\sin\left(\dfrac{\theta_B+\theta}{2}\right)}{\sin\left(\dfrac{\theta_B-\theta}{2}\right)}\right]\end{array}\right]$$
$$+\frac{1}{3\pi}\left[\begin{array}{l}(4E+12G+6F\cos\theta_B)\theta\sin\theta_B+2E\theta\cos 2\theta_B\sin\theta_B\\ +6F\sin\theta_B\sin\theta+4E\cos\theta_B\sin\theta_B\sin\theta+E\sin\theta_B\sin 2\theta\\ +3(E_2(\pi-\theta_B)+E_1\theta_B)\sin\theta\\ +6(F_2(\pi-\theta_B)+F_1\theta_B+E\sin\theta_B)(\theta-\cos\theta\sin\theta)\\ -(E_2(\pi-\theta_B)+E_1\theta_B)\sin 3\theta\end{array}\right] \quad (28)$$

where the terms E, F, and G represent E_1-E_2, F_1-F_2, and G_1-G_2, respectively. Note that this term is proportional to the acceleration of the camberline deformation (β''). The apparent mass load distribution for the conventional TE flap case can be shown to agree with the result obtained by Postel and Leppert [8].

4. Results and discussion

Two simple and practical camberline motions, pitch and heave, provide a good example of applying the general deforming camberline results derived in the previous section. For an airfoil pitching around an axis x_a (measured from the leading edge), the shape function ψ is $\psi = x_a - x = x_a - (c/2)(1-\cos\theta)$. For a heaving airfoil, ψ is written simply as $\psi = 1$. Tables 3 and 4 present the parameters defined in the present method for the pitch and heave cases. The complete lift and load distribution equations (Eqs. (12) and (14)) resulting from this derivation agree well with the known result (pp. 262-272 of Bisplinghoff, et al. [39]).

To illustrate the capability of the general deforming camberline derivation discussed in the previous section, the results of the "Morphing – Configuration A" camberline are presented. This case is of interest to morphing aircraft design where a similar camberline deformation could be applied. The unsteady load distribution and force coefficients for this case have not been presented previously in the literature.

Figs. 1 and 2 show the quasi-steady load distribution due to the steady ($T_{0,s}$) and damping ($T_{0,d}$) components, which are obtained from Eqs. (26a) and (26b). The influence of the maximum camber location on these load distribution components is shown by comparing the results for three maximum camber location (x_B) values. Similarly, Fig. 3 shows the damping component of the apparent mass load distribution ($T_{1,d}$) due to the time-rate-of change of $\gamma_{0,d}$, which is obtained from Eqs. (15d) and (28). Figs. 1, 2 and 3 represent the only configuration-specific load distribution components required for the complete unsteady load distribution defined in Eq. (16b), since $T_{1,s}$ is equal to $T_{0,d}$ and the wake-induced component is represented by χ. Therefore, the unsteady load distribution for transient or sinusoidal motion may be determined by superimposing these load distributions.

As shown in Fig. 1, the position of peak values of the steady components accords with the position of the maximum camber. Both Fig. 2 and Fig. 3 show that the position of the maximum camber does not affect the positions of the peak values of the damping coefficients. Thus, it can be said that the positions of the peak values of the damping components of both

Table 3. Lift and pitching moment parameters for a pitching and heaving airfoil.

	PITCH (ABOUT X_A)	HEAVE
$K_{0,s}$	2π	0
$K_{0,d}$	$2\pi(3/4-x_a)$	-2π
$K_{1,s}$	$\pi/2$	0
$K_{1,d}$	$(\pi/2)(1/2-x_a)$	$-\pi/2$
$J_{0,s}$	0	0
$J_{0,d}$	$-\pi/8$	0
$J_{1,s}$	$-\pi/8$	0
$J_{1,d}$	$-(\pi/2)(5/8-x_a)$	$\pi/8$

Table 4. Load distribution parameters for a pitching and heaving airfoil.

	PITCH (ABOUT X_A)	HEAVE
$A_{0,s}$	1	0
$A_{0,d}$	$1/2-x_a$	-1
$T_{0,s}$	0	0
$T_{0,d}$	$2\sin\theta$	0
$T_{1,d}$	$(1/2)(2-4x_a-\cos\theta)\sin\theta$	$-2\sin\theta$

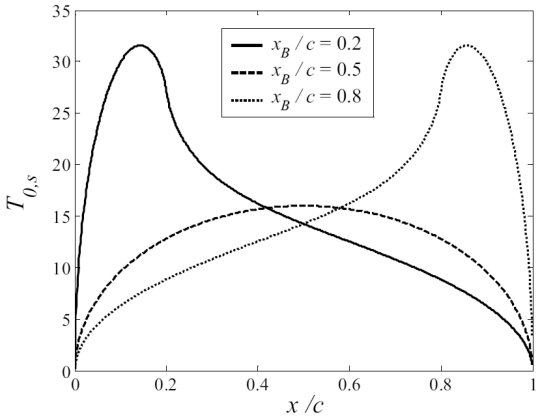

Fig. 1. Steady component of the quasi-steady load distribution for the Morphing – Configuration A camberline with various maximum camber locations.

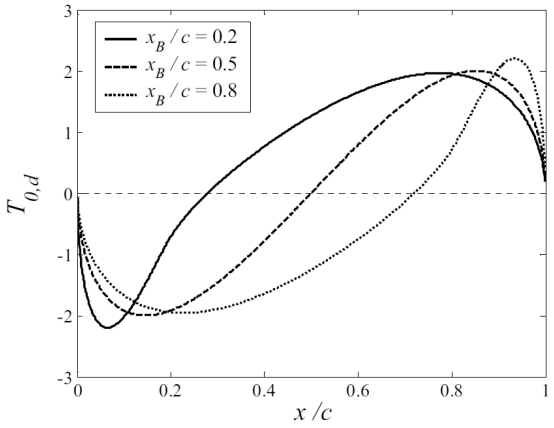

Fig. 2. Damping component of the quasi-steady load distribution for the Morphing – Configuration A case with various maximum camber locations.

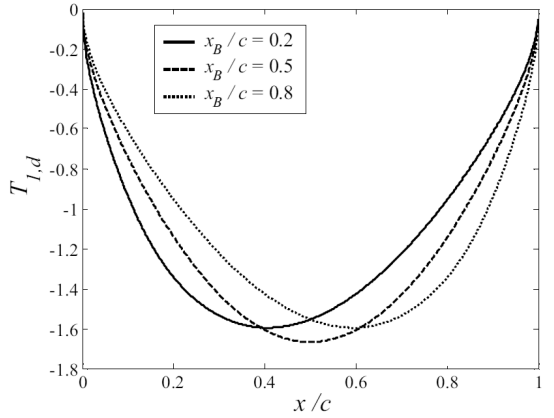

Fig. 3. Damping component of the apparent mass load distribution for the Morphing – Configuration A case with various maximum camber locations.

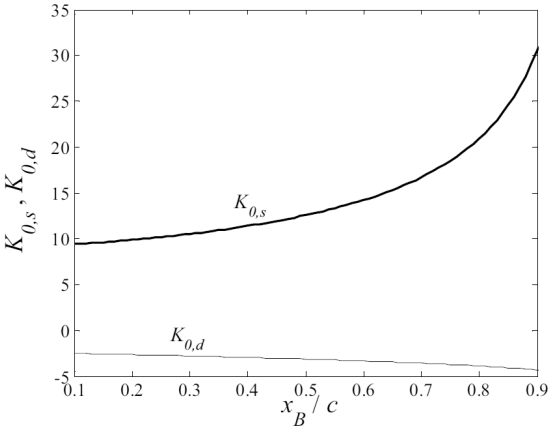

Fig. 4. Steady and damping quasi-steady lift coefficients for the Morphing – Configuration A case with various maximum camber locations.

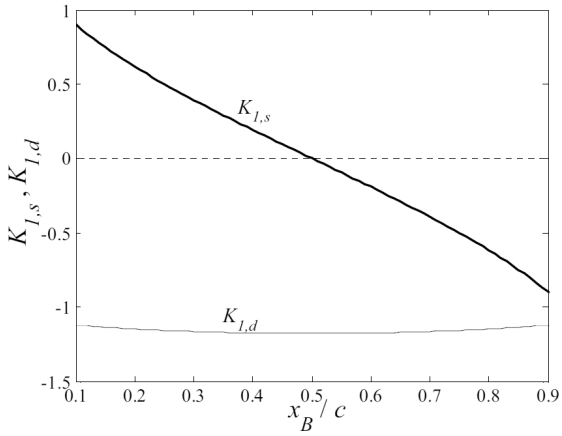

Fig. 5. Steady and damping apparent mass lift coefficients for the Morphing – Configuration A case with various maximum camber locations.

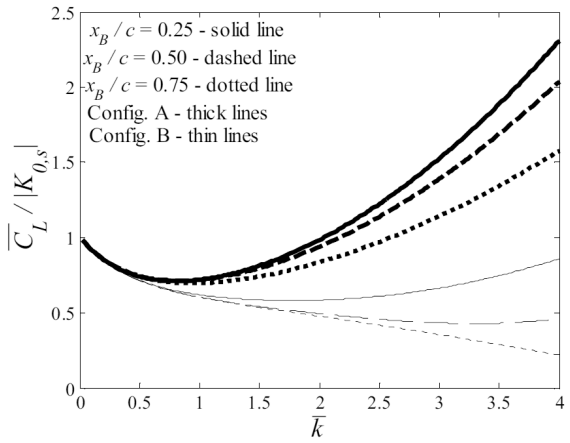

Fig. 6. Influence of the reduced frequency on the lift-coefficient magnitude for Morphing Configuration A and B.

quasi-steady and apparent mass load distributions are not much affected by the location of the maximum camber. The load distribution due to the damping aerodynamic force component is shown to be equivalent for the morphing camberline with the maximum camber located at equal distances from the airfoil center. In contrast, the load distribution due to the steady aerodynamic force term changes sign for these equivalent configurations.

Figs. 4 and 5 show the influence of the maximum camber location on the quasi-steady and apparent-mass lift components, respectively. The $K_{0,s}$ term represents the quasi-steady lift per-unit β due to the camberline shape and $K_{0,d}$ represents the quasi-steady lift per-unit $d\beta/d\tau$ generated by the rate of the camberline shape-change. Fig. 4 shows that when x_B is shifted aft the $K_{0,s}$ value increases whereas the $K_{0,d}$ term becomes more negative. For the lift components shown in Fig. 5, the $K_{1,s}$ term represents the apparent mass lift per-unit $d\beta/d\tau$ while $K_{1,d}$ represents the apparent mass lift per-unit $d^2\beta/d\tau^2$. It is seen that $K_{1,s}$ is negative for x_B/c values less than ½ while $K_{1,d}$ is negative for all x_B values. Thus, it can be said that the steady

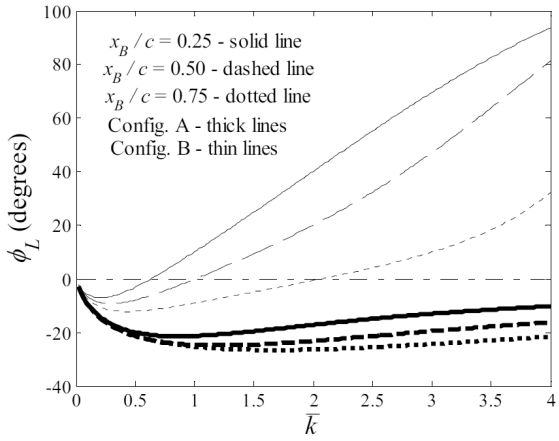

Fig. 7. Influence of the reduced frequency on the lift-coefficient phase-angle for Morphing Configuration A and B.

lift effectiveness increases for a morphing camberline as the position of maximum camber is shifted aft, while the damping lift becomes more negative.

To illustrate the application of the present approach to a sinusoidal case, the differences between the lift coefficient for the Morphing – Configuration A and Configuration B cases are presented. Fig. 6 shows the values of $C_L / |K_{0,s}|$ for these two morphing configurations. Note that $K_{0,s}$ is different for each case as shown in Fig. 4, although it is used here to normalize each case to the same oscillation in the steady-state C_L. The only difference between Configurations A and B is w_d. In fact, w_d for Configuration *B* is a combination of the w_d for Configuration *A* along with a heaving motion. The effect of maximum camber location (x_B) is seen to have a similar effect for both cases. Fig. 6 shows that the magnitude of lift is significantly larger for Configuration A. Fig. 7 presents the phase angle of the lift coefficient for the two configurations. For Configuration A, only a negative phase angle is shown while for the Configuration B the phase angle becomes positive as the reduced frequency is increased.

As shown in Figs. 6 and 7, the study of two different variable camber configurations, identified here as Configuration A and B, indicates that in the absence of camberline acceleration, the only difference between the two configurations is the magnitude of the damping additional load distribution. For a positive change in lift, the time rate of the magnitude of the camberline terms produce positive lift for Configuration B and negative lift for Configuration A. This component of the lift can have a significant effect on the maneuverability of a flight vehicle, and it is therefore a notable result. The effect of maximum camber location is seen to have a similar effect for both cases.

For oscillatory motions, the magnitude of lift is significantly larger for Configuration A for all values of reduced frequency. The phase angle for lift is positive and increases with increased reduced frequency for Configuration B, while it increases slightly, but remains negative, for Configuration A.

5. Conclusions

The unsteady thin airfoil theory for the aerodynamic analysis of deforming airfoils is derived based on the theory of von Karman and Sears for both transient and oscillatory shape changes.

It is found that the steady lift effectiveness increases for a morphing camberline as the position of maximum camber is shifted aft, while the damping lift becomes more negative. In case of the study of two different variable camber configurations, the time rate of the magnitude of the camberline terms produce positive lift for Configuration B and negative lift for Configuration A for a positive change in lift. Thus, the maneuverability of a flight vehicle of a morphing wing can be affected by the difference of morphing actuation methods. For oscillatory motions, the magnitude of lift of the Configuration A wing is significantly larger than the Configuration B wing for all the investigated values of reduced frequency.

It is expected that the convenience of the analytic pressure distributions and force coefficients obtained by the present method can be useful for fundamental studies of various morphing airfoil configurations.

Acknowledgment

The research is partially supported by Basic Science Research Program through the National Research Foundation of Korea (NRF) funded by the Ministry of Education, Science and Technology (KRF-2009-0076384) and by a grant from the Academic Research Program of Chungju National University in 2008.

Nomenclature

$\bar{A}_{n,b}$	:	Fourier coefficients defined in Eq. (13), n = 1,2,.., and *b* is the same as defined for $T_{a,b}$
c	:	Chord length
$C_{L,n}$	:	Lift coefficient, n = 0, 1, and 2 correspond to the quasi-steady, apparent mass, and wake-effect terms
$C_{M,n}$	:	Quarter-chord pitching moment coefficient, n represents the terms defined with C_L
$\bar{k}$	:	Reduced frequency defined as $\omega c/U$
L_n	:	Lift force defined in Eq. (1), n = 0, 1, and 2 corre spond to the quasi-steady, apparent mass, and wake-effect terms
q	:	Dynamic pressure
t	:	Time
$T_{a,b}$	:	Components of the aerodynamic load distribution defined in Eq. (15) , a = 0 and 1 corresponding to the quasi-steady and apparent mass terms, and $b = s$ and d corresponding to the components resulting from the steady and damping boundary condition defined in Eq. (11)
$K_{a,b}$	:	Components of the lift coefficient defined in Eq. (12), the subscripts are defined for $T_{a,b}$
U	:	Free-stream velocity

w : Induced velocity on the airfoil camberline
x : Distance along the airfoil chord aligned with the free-stream velocity
x_B : Location along the airfoil where the two segments of the general deforming camberline connect
Z_n : Components of the oscillatory lift coefficient defined in Eq. (21)
α : Angle of attack
β : Defines the time-history of the camberline shape change
χ : Shape of an angle of attack load distribution defined under Eq. (15)
$\Delta C_{p,n}$: Nondimensional unsteady pressure loading, n = 0, 1, and 2 correspond to the quasi-steady, apparent mass, and wake-effect terms
Δp_n : Unsteady pressure loading defined in Eq. (5), n = 0, 1, and 2 correspond to the quasi-steady, apparent mass, and wake-effect terms
γ_{0c} : Circulatory quasi-steady vorticity distribution
γ_{0nc} : Noncirculatory quasi-steady vorticity distribution
Π_n : Components of the oscillatory load distribution defined in Eq. (23)
θ : Polar coordinate along the airfoil surface
τ : Nondimensional time
ψ : Shape function of the airfoil camberline defined in Eq. (10)
ω : Frequency

References

[1] E. Forster, B. Sanders and F. Eastep, Synthesis of a variable geometry trailing edge control surface, AIAA paper 2003-1717, April 2003.

[2] E. Forster, B. Sanders and F. Eastep, Modeling and sensitivity analysis of a variable geometry trailing edge control surface, AIAA paper 2003-1807, April 2003.

[3] E. Stanewsky, Aerodynamic benefits of adaptive wing technology, *Aerospace Sciences and Technology*, 4 (2000) 439-452.

[4] C. O. Johnston, *et al*., Actuator-work concepts applied to unconventional control devices, *Journal of Aircraft*, 44 (2007) 1459-1468.

[5] C. O. Johnston, *et al*., A model to compare the flight control energy requirements of morphing and conventionally Actuated wings, AIAA paper 2003-1716 (2003).

[6] T. Theodorsen, General theory of aerodynamic instability and the mechanism of flutter, NACA Report No. 496 (1935).

[7] T. von Karman and W. R. Sears, Airfoil theory for non-uniform motion, *Journal of the Aeronautical Sciences*, 5 (10) August, (1938) 378-390.

[8] E. E. Postel and E. L. Leppert, Theoretical pressure distribution for a thin airfoil oscillating in incompressible flow, *Journal of the Aeronautical Sciences*, 15 (8) August (1948) 486-492.

[9] F. Dietze, The air forces on a harmonically oscillating self-deforming plate, *Luftfarhtforschung*, 16 (2) (1939) 84.

[10] F. Dietze, Law of aerodynamic force of a jointed plate in harmonic motion, *Luftfarhtforschung*, 18 (4) (1941) 135.

[11] F. Dietze, Comparative calculations concerning aerodynamic balance of control surfaces, in *Three Papers from Conference on Wing and Tail Surface Interactions*, (Translated from Lilienthal-Gesellschaft fur Luftfahrtforschung, March 1941, pp. 61-74, NACA TM 1306 (1951).

[12] K. Jaekel, On the calculation of the circulation distribution for a twod-dimensional wing having periodic motion, *Luftfarhtforschung*, 16 (3) (1939) 135.

[13] L. Schwarz, Calculation of the pressure distribution of a wing harmonically oscillating in two-dimensional flow, *Luftfarhtforschung*, 17 (11) (1940) 379.

[14] L. Schwarz, Aerodynamically equivalent systems for various forms of control surfaces within the scope of the two-dimensional wing theory, in *Three Papers from Conference on Wing and Tail Surface Interactions*, (Translated from Lilienthal-Gesellschaft fur Luftfahrtforschung, March 1941, pp. 61-74), NACA TM 1306 (1951).

[15] H. Sohngen, Remarks concerning aerodynamically balanced control surfaces, in *Three Papers from Conference on Wing and Tail Surface Interactions*, (Translated from Lilienthal-Gesellschaft fur Luftfahrtforschung, March 1941, pp. 61-74), NACA TM 1306 (1951).

[16] H. Sohngen, Determination of the lift distribution for optionally non-uniform movement, *Luftfarhtforschung*, 17 (11) (1940) 401.

[17] D. Mateescu and M. Abdo, Unsteady aerodynamic solutions for oscillating airfoils, AIAA paper 2003-227 (2003).

[18] J. P. Narkiewicz, A. Ling and G. T. S. Done, Unsteady aerodynamic loads on an aerofoil with a deflecting tab, *Aeronautical Journal*, August/ September (1995) 282-292.

[19] J. G. Leishman, Unsteady lift of a flapped airfoil by indicial concepts, *Journal of Aircraft*, 31 (2) March-April (1994) 288-297.

[20] N. Hariharan and J. G. Leishman, Unsteady aerodynamics of a flapped airfoil in subsonic flow by indicial concepts, *Journal of Aircraft*, 33 (5) March-April (1996) 855-868.

[21] B. Sanders, F. E. Eastep and E. Forster, Aerodynamic and aeroelastic characteristics of wings with conformal control surfaces for morphing aircraft," *Journal of Aircraft*, 40 Jan.-Feb. (2003) 94-99.

[22] E. Forster, B. Sanders and F. Eastep, Modeling and sensitivity analysis of a variable geometry trailing edge control surface, AIAA paper 2003-1807, April 2003.

[23] I. E. Garrick, Nonsteady wing characteristics, in *Aerodynamic Components of Aircraft at High Speeds*, Vol. VII of *High Speed Aerodynamics and Jet Propulsion*, edited by Donovan, A. F., and Lawrence, H. R. (1957).

[24] I. N. Spielburg, The two-dimensional incompressible aerodynamic coefficients for oscillatory changes in airfoil camber, *Journal of the Aeronautical Sciences*, 20 (6) June (1953) 432-433.

[25] M. Mesaric and F. Kosel, Unsteady airload of an airfoil

with variable camber, *Aerospace Science and Technology*, 8 (2004) 167-174.
[26] J. Singh, Unsteady aerodynamics of deforming airfoils – A theoretical and numerical study, AIAA paper 96-2162 (1996).
[27] B. J. Maclean and R. A. Decker, Lift analysis of a variable camber foil using the discrete vortex blob method, *AIAA Journal*, 32 (7) July (1994) 1525-1527.
[28] R. P. Llewelyn, The velocity distribution on a polynomial mean line and the converse, *Journal of the Royal Aeronautical Society*, 68 (1964) 57-58.
[29] E. A. Boyd, Comment on a conjecture of tanner, *Journal of the Royal Aeronautical Society*, 67 (1963) 127-129.
[30] E. A. Boyd, Generalisation of the condition for waviness in the pressure distribution on a cambered plate, *Journal of the Royal Aeronautical Society*, 67 (1963) 529-530.
[31] E. A. Boyd, Comment on the "The load distribution on a polynomial mean line and the converse," *Journal of the Royal Aeronautical Society*, 68 (1964) 59.
[32] H. Glauert, *The Elements of Aerofoil and Airscrew Theory*, 2nd Edition, Cambridge University Press (1947).
[33] H. J. Allen, General theory of airfoil sections having arbitrary shape or pressure distribution, NACA Report No. 833, 1943.
[34] S. Neumark, Pressure distribution on an airfoil in nonuniform motion, *Journal of the Aeronautical Sciences*, 19 (3) March (1952) 214-215.
[35] R. T. Jones, The unsteady lift of a wing of finite aspect ratio, NACA Report No. 681 (1940).
[36] D. A. Spence, The lift on a thin airfoil with a jet-augmented flap, *Aeronautical Quarterly*, 9 Aug. (1958) 287-299.
[37] C. O. Johnston, Actuator-Work Concepts Applied to Morphing and Conventional Aerodynamic Control Devices, M.S. Thesis, Virginia Tech (2003).
[38] R. M. Pinkerton, Calculated and measured pressure distributions over the midspan section of the NACA 4412 airfoil, NACA Report No. 563 (1936).
[39] R. L. Bisplinghoff, H. Ashley and R. L. Halfman, *Aeroelasticity*, Addison-Wesley (1955).

Christopher O. Johnston is currently2 an Aerospace Engineer in the Aerothermodynamics Branch at NASA Langley Research Center. He received his B.S., M.S., and Ph.D. at Virginia Tech, which is where the present work was performed.

Cheolheui Han received a B.S. degree in Mechanical Engineering from Hanyang University in 1993. He received his M.S. and Ph.D. degrees from Hanyang University in 1998 and 2003, respectively. Then, he worked as a visiting post-doctoral researcher at the Dept. of Aerospace and Ocean Engineering at Virginia Tech, USA. Dr. Han is currently an Assistant Professor at the Department of Aeronautical and Mechanical Design Engineering.